Galactic cannibalism and cold dark matter density profiles

C. Nipoti,[1]★ T. Treu,[2]† L. Ciotti[3] and M. Stiavelli[4]

[1]*Theoretical Physics, Oxford University, 1 Keble Road, Oxford OX1 3NP*
[2]*Department of Physics and Astronomy, UCLA, Box 951547, Los Angeles, CA 90095-1547, USA*
[3]*Department of Astronomy, Bologna University, via Ranzani 1, 40127 Bologna, Italy*
[4]*Space Telescope Science Institute, 3700 San Martin Drive, Baltimore, MD 21218, USA*

ABSTRACT

Using *N*-body simulations, we show that the process of formation of the brightest cluster galaxy through dissipationless galactic cannibalism can affect the inner cluster dark matter density profile. In particular, we use as a realistic test case the dynamical evolution of the galaxy cluster C0337−2522 at redshift $z = 0.59$, hosting in its centre a group of five elliptical galaxies which are likely to be the progenitor of a central giant elliptical. After the formation of the brightest cluster galaxy, the inner cluster dark matter density profile is significantly flatter (logarithmic slope $0.49 \lesssim \beta \lesssim 0.90$) than the original cusp ($\beta = 1$), as a consequence of dynamical friction heating of the massive galaxies against the diffuse cluster dark matter. In our simulations we have assumed that the cluster galaxies are made of stars only. We also show that the presence of galactic dark matter haloes can steepen the cluster central density profile. We conclude that galactic cannibalism could be a viable physical mechanism to reconcile – at least at the cluster scale – the flat dark matter haloes inferred observationally in some galaxy clusters with the steep haloes predicted by cosmological simulations.

Key words: galaxies: clusters: general – galaxies: elliptical and lenticular, cD – dark matter.

1 INTRODUCTION

Cold dark matter (CDM) cosmological simulations predict that the inner density profile of dark matter (DM) haloes is characterized by a cusp: $\rho_{\rm DM}(r) \propto r^{-\beta}$, with logarithmic slope $\beta \sim 1$–1.5 for $r \to 0$; the exact value of the slope and its universality are at the centre of a lively debate. For example, several authors (Navarro, Frenk & White 1996, hereafter NFW; Moore et al. 1998; Ghigna et al. 2000; Navarro et al. 2004) claim that the resulting profiles are universal, in the sense that β is independent of the halo mass. Other authors suggest that the inner profile depends significantly on the slope of the power spectrum, so that the higher the mass of the halo, the steeper the cusp (Subramanian, Cen & Ostriker 2000; Ricotti 2003, and references therein).

These predictions have been extensively tested by observations both in galaxies (e.g. Salucci & Burkert 2000; van den Bosch et al. 2000; de Blok et al. 2001; Simon et al. 2003) and in clusters of galaxies (e.g. Smith et al. 2001; Sand, Treu & Ellis 2002; Kelson et al. 2002; Gavazzi et al. 2003; Lewis, Buote & Stocke 2003; Sand et al. 2004). The derived values of β range from $\sim$0 to $\sim$1.3. The observational results – shallow slopes and intrinsic scatter – could represent a serious challenge to the standard cosmological model,

and exotic scenarios have been also proposed to solve this problem (e.g. Spergel & Steinhardt 2000).

In any case, the role of baryons must be better understood before we are forced to reject a successful paradigm. In fact, it is well known that on scales of the order of kiloparsec, baryons are important and their evolution may affect substantially the DM distribution (see Binney 2004 for a discussion). For example, in the so-called 'adiabatic contraction' approximation (Blumenthal et al. 1986; Gnedin et al. 2004), baryon dissipation effectively steepens the inner density profile of the host halo (Mo, Mao & White 1998; Kochanek & White 2001), thus exacerbating the contrast between theory and observations.

Here, motivated by recent observational studies of galaxy clusters based on a joint lensing and dynamical analysis – in which Sand et al. (2002, 2004) report inner logarithmic slopes in the range[1] $\beta = 0.38$–0.99 – we focus on the cluster-sized DM haloes, which are considered to be less affected by baryon dissipation, with respect to galaxy-sized haloes.

We note that the spiralling in of massive galaxies in clusters could flatten the cluster DM distribution, by heating it through dynamical

---

[1] The uncertainties on β could be higher than those given by Sand et al. (2004) if the ellipticity of the cluster mass distribution is higher than estimated by the authors (cf. Bartelmann & Meneghetti 2004; Dalal & Keeton 2004). Additional observational work is currently under way to clarify those issues and measure the distribution of DM inner slopes for larger samples of clusters.

★E-mail: nipoti@thphys.ox.ac.uk
†Hubble fellow.

© 2004 RAS

friction (similar to the galaxy–globular cluster interaction at smaller scales; see Bertin, Liseikina & Pegoraro 2003). Recently, El-Zant et al. (2004), using *N*-body simulations, found that dynamical friction heating due to galaxies, modelled as rigid baryon clumps, is indeed effective in flattening the inner DM profile in clusters. Similar conclusions, in a different context, were also reached by Ma & Boylan-Kolchin (2004), who explored with *N*-body simulations the effects of the dynamical evolution of (deformable) DM subhaloes on the DM distribution of their host halo. On the other hand, the mass infall associated with the spiralling in of the galaxies towards the cluster centre deepens the central potential well. This dissipationless contraction, in contrast with dynamical friction heating, can result in shrinking the cluster DM distribution and steepening its inner density profile (see, for example, Barnes & White 1984; Jesseit, Naab & Burkert 2002): the final density profile will be the result of the two competing effects (see also Section 4).

Here we investigate the effects of dynamical friction on the cluster DM distribution in a realistic scenario, by simulating the time evolution of the galaxy cluster C0337−2522 at redshift $z = 0.59$ (*ROSAT* Deep Cluster Survey; Rosati et al. 1998). This cluster is characterized by the presence of five bright elliptical galaxies (Es) located within ∼30 kpc from the centre, in projection. Nipoti et al. (2003b, hereafter N03), using *N*-body simulations, have shown that the five galaxies are very likely to merge and form a brightest cluster galaxy (BCG) by $z = 0$, in accordance with the predictions of the galactic cannibalism scenario (Ostriker & Tremaine 1975; see also Merritt 1983; Dubinski 1998). In the present work we consider the evolution of the underlying cluster DM distribution, with the aid of additional higher-resolution simulations (see also Nipoti et al. 2003c). In our models the single galaxies, as well as the cluster DM, are represented by *N*-body distributions. This is particularly important because tidal stripping could remove mass from the individual galaxies, thus altering the infall process and its effects on the cluster DM halo.

2 NUMERICAL SIMULATIONS

2.1 Initial conditions

Our simulations represent possible realizations of the dynamical evolution of C0337−2522 – a poor galaxy cluster, with five bright Es in its centre – from redshift $z = 0.59$ to the present. The observational data and the set-up of the initial conditions are described in detail in N03.

In the initial conditions of the simulations, the cluster is represented as a live spherically symmetric DM distribution, hosting five identical massive galaxies modelled as spherical *N*-body systems. For simplicity, we only consider simulations where each galaxy is represented by a single collisionless component (stars). This is justified under the assumption that the mass of the galaxies in the cluster centre is dominated by luminous matter (e.g. Treu & Koopmans 2004), and that the extended DM halo is likely to be tidally stripped in the innermost region of the cluster (e.g. Natarajan, Kneib & Smail 2002).

2.2 Models

For the cluster DM distribution we use a Hernquist (1990) model

$$\rho_{cl}(r) = \frac{M_{cl} r_{cl}}{2\pi r (r_{cl} + r)^3}, \tag{1}$$

where M_{cl} and r_{cl} are cluster total mass and break radius, respectively. Thus, $\rho_{cl}(r) \sim r^{-1}$ for $r \to 0$, as in the NFW density profile; but, unlike the NFW profile, the total mass is finite because $\rho_{cl}(r) \sim r^{-4}$ for $r \to \infty$. In the simulations the distribution function of the cluster has been chosen isotropic or radially anisotropic (see N03); r_{cl} is either 100 or 300 kpc, and the total cluster mass is in the range 4.8×10^{13} to 3.06×10^{14} M$_\odot$ (see Table 1).

At the beginning of each simulation the five galaxies are identical (isotropic or radially anisotropic) Hernquist models; their stellar density distribution ρ_* is described by equation (1), with break radius $r_* \simeq 2.2$ kpc and total mass $M_* = 4 \times 10^{11}$ M$_\odot$. The initial centre-of-mass positions and velocities of the five galaxies are chosen by extraction from the cluster distribution function, constrained by the observational data (see N03). Note that simulations with the same cluster parameters (namely, the pairs of simulations 5a and 6, 18 and 19, 20 and 21; see Table 1) differ in the initial centre-of-mass positions and velocities of the galaxies. In simulations 1s and 1s.1 we consider an additional population of 50 smaller galaxies (each modelled as a Hernquist model with $M_* = 5 \times 10^{10}$ M$_\odot$ and $r_* \simeq 0.55$ kpc) distributed in phase-space according to the cluster distribution function (see Fig. 1, left panel).

The total time of each simulation is ∼6.1 Gyr, of the order of $100 \, T_{dyn}$, where T_{dyn} is the half-mass dynamical time of the initial galaxy models (we adopt $\Omega_m = 0.3$, $\Omega_\Lambda = 0.7$ and $H_0 = 65$ km s^{-1} Mpc^{-1}).

Table 1. Parameters of the simulations. The first column gives the name of the simulation. r_{cl} is the initial cluster break radius (kpc). M_{cl} is the cluster mass (10^{13} M$_\odot$). N_{DM} is the total number of DM particles. N_{lum} is the total number of stellar particles. $r_{DM,f}/r_{cl}$ is the best-fitting break radius of the final DM profile normalized to the initial break radius. β is the best-fitting logarithmic slope of the final DM profile. 1σ uncertainties on $r_{DM,f}/r_{cl}$ and β are reported. Simulations 1.1, 1s.1, 3.1, 17.1 and 20.1 are higher-resolution replicas of simulations 1, 1s, 3, 17 and 20, respectively. Pairs of runs with the same cluster parameters (5a and 6, 18 and 19, 20 and 21) differ in the initial centre-of-mass positions and velocities of the galaxies. In simulations 1s and 1s.1 50 small galaxies are added.

| Simulation	r_{cl}	M_{cl}	N_{DM}	N_{lum}	$r_{DM,f}/r_{cl}$	β
1	100	4.8	235 520	10 240	$0.77^{+0.04}_{-0.04}$	$0.50^{+0.09}_{-0.09}$
1s	100	4.8	222 720	23 040	$0.75^{+0.04}_{-0.04}$	$0.49^{+0.07}_{-0.07}$
3	100	5.3	130 560	5120	$0.91^{+0.03}_{-0.03}$	$0.89^{+0.04}_{-0.04}$
5a	100	9.6	120 320	2560	$0.79^{+0.04}_{-0.04}$	$0.59^{+0.08}_{-0.08}$
6	100	9.6	120 320	2560	$0.77^{+0.04}_{-0.04}$	$0.52^{+0.08}_{-0.07}$
7	100	10.6	266 240	5120	$0.83^{+0.04}_{-0.04}$	$0.68^{+0.06}_{-0.06}$
14a	300	13.5	170 240	2560	$0.93^{+0.03}_{-0.03}$	$0.90^{+0.06}_{-0.05}$
17	300	15.3	193 280	2560	$0.84^{+0.05}_{-0.04}$	$0.72^{+0.08}_{-0.08}$
18	300	27.0	171 520	1280	$0.91^{+0.03}_{-0.03}$	$0.86^{+0.05}_{-0.05}$
19	300	27.0	171 520	1280	$0.86^{+0.05}_{-0.04}$	$0.76^{+0.08}_{-0.08}$
20	300	30.6	194 560	1280	$0.89^{+0.05}_{-0.05}$	$0.81^{+0.06}_{-0.06}$
21	300	30.6	194 560	1280	$0.91^{+0.03}_{-0.03}$	$0.85^{+0.05}_{-0.05}$
1.1	100	4.8	942 080	40 960	$0.76^{+0.04}_{-0.04}$	$0.51^{+0.08}_{-0.08}$
1s.1	100	4.8	890 880	92 160	$0.74^{+0.04}_{-0.04}$	$0.49^{+0.09}_{-0.09}$
3.1	100	5.3	1 044 480	40 960	$0.90^{+0.05}_{-0.05}$	$0.89^{+0.08}_{-0.08}$
17.1	300	15.3	773 120	10 240	$0.84^{+0.04}_{-0.04}$	$0.72^{+0.08}_{-0.09}$
20.1	300	30.6	1 556 480	10 240	$0.90^{+0.05}_{-0.05}$	$0.83^{+0.06}_{-0.07}$

© 2004 RAS, MNRAS **355**, 1119–1124
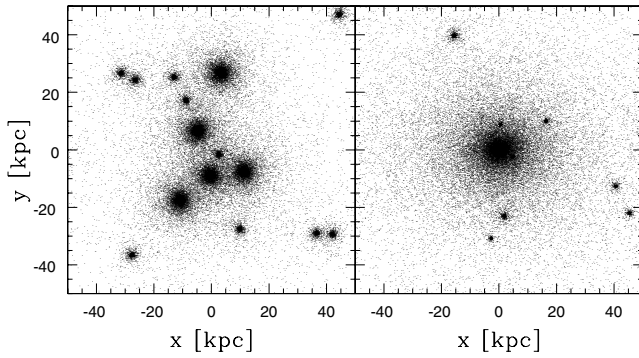
Figure 1. Simulation 1s.1: snapshots of the initial ($z = 0.59$, left) and final ($z = 0$, right) projected distribution of the stellar particles in the inner cluster region.

2.3 Codes and numerical tests

For most of the numerical N-body simulations (the first 12 listed in Table 1) we used the Springel, Yoshida & White (2001) GADGET code, with cell-opening parameter $\alpha = 0.02$, minimum and the maximum time-step $\Delta t_{min} = 0$ and $\Delta t_{max} = T_{dyn}/100$, time-step tolerance parameter $\alpha_{tol} = 0.05$ and softening parameter $\varepsilon \simeq 0.36 r_*$. Additional higher-resolution simulations (1.1, 1s.1, 3.1, 17.1, 20.1) were obtained using the parallel code FVFPS (FORTRAN version of a fast Poisson solver; Londrillo, Nipoti & Ciotti 2003). This code, based on algorithms introduced by Dehnen (2002), has been successfully tested and compared with GADGET (Nipoti 2003; Nipoti, Londrillo & Ciotti 2003a). In particular, we adopted the following values of the parameters: minimum value of the opening parameter $\theta_{min} = 0.5$; softening parameter $\varepsilon \simeq 0.1 r_*$; initial time-step $\Delta t \sim T_{dyn}/100$. In all simulations, stellar and DM particles have the same mass, and the total energy is conserved within 1 per cent.

Discreteness, two-body relaxation and softening are expected to artificially alter the very inner DM density profile. To quantify numerical effects, we have run a few test simulations where the initial conditions are represented by the cluster DM halo only, for the adopted codes and values of the parameters (softening, number of DM particles, time-step, opening parameter, total elapsed time). The final profile of one of these test simulations (with the same parameters as simulation 1.1) is shown in Fig. 2 (open symbols). In all the test simulations, the Hernquist profile is preserved for $r \gtrsim 0.05 r_{cl}$. Thus, we only consider the properties of the cluster DM halo for $r \gtrsim 0.05 r_{cl}$ in the analysis of all the presented simulations. We note that in the initial conditions of the lowest resolution of our simulations $r \sim 0.05 r_{cl}$ contains $\sim$270 particles. Thus, our choice of the minimum reliable radius is consistent with recent numerical convergence studies (Power et al. 2003, and references therein).

Other possible numerical artefacts might be due to the small number of particles used to represent each galaxy (128–2048, in the simulations run with GADGET). In particular, it is likely that in our simulations we overestimate the galaxy mass that is tidally stripped (see Kazantzidis et al. 2004) and this might affect the response of the cluster DM. To explore this problem we ran simulations 1.1, 1s.1, 3.1, 17.1 and 20.1, which have the same initial conditions as simulations 1, 1s, 3, 17 and 20, respectively, but a higher total number of particles ($\sim$10^6 DM particles, and 2048–8192 stellar particles for each of the five galaxies). We checked that all the relevant properties of the system evolve in the same way in the corresponding higher- and lower-resolution simulations. In particular, the final cluster DM profile is practically indistinguishable in the two cases over the considered radial range $r \gtrsim 0.05 r_{cl}$.
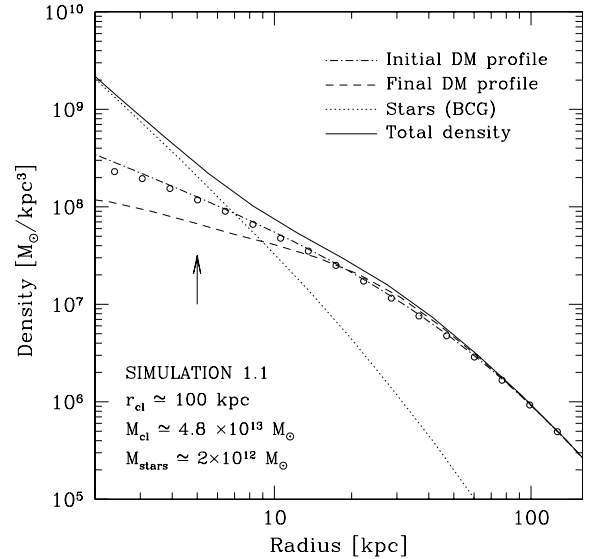
Figure 2. Final density distribution of the cluster dark, luminous and total matter in simulation 1.1. The dot–dashed curve is the initial (Hernquist) DM profile. The arrow indicates the minimum radius considered for the fit. Open symbols refer to a test simulation run to exclude numerical artefacts (see Section 2.3).

3 RESULTS

In all the simulations, three to five of the five massive galaxies merge before $z = 0$ at the bottom of the cluster potential well, as a consequence of dynamical friction. Fig. 1 shows, as an example, the initial ($z = 0.59$, left) and final ($z = 0$, right) projected distributions of the stellar particles in the inner $\sim$50 kpc for simulation 1s.1. In any case, the merger remnant is similar in its main structural and dynamical properties to a real BCG (see N03). Here we discuss the effects of this dissipationless multiple merging event on the underlying cluster DM distribution.

3.1 Properties of the final dark matter density profile

To quantify the combined effects of dynamical friction heating and dissipationless contraction, we fit the final angle-averaged DM density profile using a generalization of the Hernquist profile, in the form (Dehnen 1993)

$$\rho_{DM}(r) = \frac{\rho_{DM,0} r_{DM}^4}{r^\beta (r_{DM} + r)^{4-\beta}}, \tag{2}$$

where the inner slope β and the break radius r_{DM} are free parameters, and the reference density $\rho_{DM,0}$ is constrained by the total DM mass. The initial cluster DM density profile (equation 1) corresponds to the case $\beta = 1$, $r_{DM} = r_{cl}$, and $\rho_{DM,0} = M_{cl}/(2\pi r_{cl}^3)$. When computing the angle-averaged density profile of the final DM distribution, we determine the centre of the cluster using the iterative technique described by Power et al. (2003): the centre of mass of the system is computed recursively, considering particles within a sphere whose radius shrinks by 2.5 per cent at each step. We stop the iteration when the sphere contains $\sim$1000 particles.[2] The best-fitting β and

---

[2] As a check, we also computed the centre of the system as the position of the lowest-potential energy particle, finding good agreement with the adopted method.

$r_{\rm DM}$ for the final cluster DM distribution of each simulation are reported in Table 1; 1σ uncertainties on the best-fitting parameters are calculated from $\Delta\chi^2 = 2.30$ contours in the space β–$r_{\rm DM}$.

Fig. 2 shows the final dark, luminous and total matter distribution for simulation 1.1: the final cluster DM distribution (dashed line) is centrally shallower than the initial Hernquist profile (dot–dashed line). The modification is apparent at $r \lesssim 20$ kpc, where the contribution of the newly formed central galaxy (dotted line) to the total density (solid line) becomes relevant. Thus, the central cluster DM cusp after the formation of the BCG is flatter than the original $\rho_{\rm DM} \propto r^{-1}$.

We find the same qualitative behaviour of the final luminous and DM distributions in all the other simulations, although simulation 1.1 represents one of the cases where flattening is more effective (the final best-fitting β is ~ 0.5). Considering all of our simulations, we find best-fitting logarithmic slope β in the range $0.49 \lesssim \beta \lesssim 0.90$, with average $\langle\beta\rangle = 0.71$. Comparing the best-fitting final break radius $r_{\rm DM,f}$ with the break radius $r_{\rm cl}$ of the corresponding initial Hernquist model, we find $0.74 \lesssim r_{\rm DM,f}/r_{\rm cl} \lesssim 0.95$, with average $\langle r_{\rm DM,f}/r_{\rm cl}\rangle = 0.85$. We note that the best-fitting final break radius is not a direct measure of the concentration of the system, because it can be significantly affected by the change in the shape of the density distribution. In fact, the final radii containing 10, 50, 70 and 90 per cent of the total DM mass are always larger than 95 per cent of the corresponding initial values, even for quite small $r_{\rm DM,f}/r_{\rm cl}$ (e.g. simulations 1 and 1s). Thus, in our models, deviations of $r_{\rm DM,f}$ from $r_{\rm cl}$ indicate a difference in the shape of the profile, as does the value of β.

Simulation 1s.1 has the same initial conditions (cluster mass, radius and distribution function, and phase-space coordinates of the centres of mass of the galaxies) as simulation 1.1, but in the first case 50 smaller galaxies are added to the five massive galaxies to represent the cluster population (see Fig. 1). We find that the main properties of the final matter distribution in simulation 1s.1 are not significantly different from those of simulation 1.1. We conclude that even a rather simple model, representing only the more massive galaxies in the initial conditions, is sufficient to capture the main physical processes.

Thus, in the considered scenario we find that the most important effect of the formation of a BCG through galactic cannibalism on the underlying diffuse DM distribution is to produce a shallower final cluster DM distribution. In other words, dynamical friction heating is more effective than contraction due to the mass infall.

3.2 Physical interpretation

In Fig. 3 we plot the final best-fitting β (top) and $r_{\rm DM,f}/r_{\rm cl}$ (bottom) as a function of the ratio $M_{\rm lum}/M_{\rm cl}$ between the total mass in stars and the total cluster mass (DM plus stars). The general trend is that the final density profile is shallower when $M_{\rm lum}/M_{\rm cl}$ is higher. However, the distribution of points in the plane $M_{\rm lum}/M_{\rm cl}$–β (as well as in the plane $M_{\rm lum}/M_{\rm cl}$–$r_{\rm DM,f}/r_{\rm cl}$) is characterized by a significant scatter. For example, simulations 1 and 3 have roughly the same $M_{\rm lum}/M_{\rm cl} \sim 0.04$, but significantly different final inner slopes ($\beta \sim 0.5$ and $\beta \sim 0.9$, respectively). This suggests that the cluster mass is not a discriminant in determining the final density profile. We argue that the orbital properties of the five galaxies represent the main factor affecting the final slope of the DM cusp. This picture would be consistent with our findings, because simulations with the same or similar $M_{\rm lum}/M_{\rm cl}$ (and cluster break radius) differ only in the initial phase-space coordinates of the galaxies in the cluster. In general, galaxies on different orbits will heat the underlying DM at
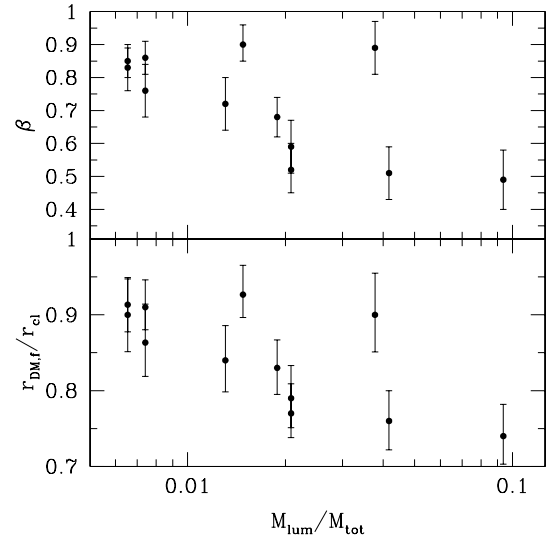

Figure 3. Best-fitting logarithmic inner slope β (top) and break radius $r_{\rm DM,f}$ (normalized to the initial break radius; bottom) of the final DM density distribution versus the ratio between the total mass in stars and total cluster mass (DM plus stars). Bars indicate 1σ uncertainties.

different radii and at different rates. Thus, it is not surprising to find a range of values of β in simulations with similar cluster parameters, but different initial positions and velocities of the galaxies.

In order to quantify this effect, we present here the results of a very simple exercise. We ran two additional test simulations, with the same number of particles, cluster parameters and initial positions of the five galaxies as simulation 1, but different initial velocities. In one case, each galaxy starts with half the initial kinetic energy it has in simulation 1 (and the same direction of the velocity vector); in the other, the galaxies have null initial velocities. Interestingly, we find best-fitting final slopes $\beta \simeq 0.68$ in the former case, and $\beta \simeq 1.29$ in the latter, to be compared with $\beta \simeq 0.50$ for simulation 1. In other words, for fixed initial position of a galaxy, the smaller its initial kinetic energy is, the smaller the amount of energy it transfers to the cluster DM through dynamical friction heating. We also recall that the infall of the galaxies into the cluster centre deepens the cluster gravitational potential well. If the amount of dynamical friction heating is quite small (as in the extreme case of the test simulation in which the galaxies start at rest), then dissipationless contraction dominates and the final cusp is steeper than the initial.

We conclude that the orbital parameters of the galaxies are important in determining the final DM distribution, as clearly illustrated by the results of the two test simulations presented above. However, it must be stressed that these test simulations – intended only to isolate an important physical effect – are characterized by quite artificial initial conditions, which are not extracted from a distribution function and are not consistent with the observational phase-space constraints considered in our work (see N03).

3.3 Comparison with observations

How do the results of our simulations compare with observationally determined cluster DM density profiles? The galaxy clusters observed by Sand et al. (2004) are suitable for this type of exercise. These clusters (MS2137−23, Abell 383, RXJ1133, Abell 963, MACS1206, A1201) are at redshifts lower than that of C0337−2522, they have total mass of the order of a few 10^{14} M$_\odot$,

and they host a dominant giant elliptical (with mass around 10^{12} M$_\odot$) apparently relaxed at the bottom of the cluster potential well. Sand et al. (2004) found slopes $0.38 \lesssim \beta \lesssim 0.99$ with an average value of $\langle \beta \rangle \sim 0.52$ for the first three clusters, and an upper limit $\beta < 0.57$ for the others. It appears that our simulations are able to reproduce their observations. In particular, it is interesting to compare the final matter distribution of simulation 1.1 with the best-fitting model which Sand et al. found for MS2137−23 (cf. Fig. 2 with their fig. 7). The similarity of the DM and stellar distributions is striking: the best-fitting slope is $\beta = 0.57$ for MS2137−23 and $\beta = 0.50$ for the end-product of simulation 1.1. Not only can the proposed mechanism reconcile the shallow observed slopes with the steep slopes obtained in DM-only simulations, but also the various realizations of the cannibalism process could introduce additional scatter, thus helping to explain the observed scatter.

Ultimately, when more observations are available and we can measure the distribution of the final slopes, it might be possible to use the observed scatter to constrain the history of cannibalism in clusters.

4 SUMMARY AND CONCLUSIONS

In this paper we have explored, with the aid of *N*-body simulations, the effects on the inner cluster DM density profile of the formation of a BCG, through dissipationless multiple merging of pre-existing galaxies. The initial conditions are designed to reproduce the observed galaxy cluster C0337−2522 ($z = 0.59$). Although we focus on a single well-observed system as a case study, we stress that the results of the simulations could be generalized to poor galaxy clusters where the central giant elliptical was formed as a consequence of galactic cannibalism, with negligible dissipation.

We have found that the inner cluster DM profile is sensitive to the dynamical evolution of cluster galaxies, and in particular to the formation of a BCG. In our models, where the initial condition are realistic and the galaxies are deformable, we find final slopes in the range $0.49 \lesssim \beta \lesssim 0.90$, with average $\langle \beta \rangle = 0.71$. The qualitative behaviour of our simulations is in agreement with that found by El-Zant et al. (2004), although they obtained quite a small value of the final inner slope ($\beta \simeq 0.35$), which is likely to be due to the use of rigid clumps, combined with a high fraction of luminous (clumped) matter ($M_{\rm lum}/M_{\rm cl} \simeq 0.06$). Dynamical friction heating in a cluster with original inner density profile $\rho_{\rm DM} \propto r^{-1}$ can thus produce a flatter final inner slope for the cluster DM. Recent measures of the DM profiles of observed clusters can be interpreted taking into account this mechanism.

As outlined in the introduction, our results are based on the assumption that cluster galaxies are essentially made of stars. However, in a scenario in which the contribution of galactic DM haloes to galaxy masses is important, the inspiralling galaxies might bring a significant amount of DM in the centre of the cluster. For instance, if we consider, as an extreme case, that the massive galaxies in our simulations are made of DM only, the final DM cusp would be steeper than r^{-1}, because the DM infall is dominant over dynamical friction heating (see the solid curve in Fig. 2). A similar scenario has been recently considered by Ma & Boylan-Kolchin (2004), who studied the interplay between a DM halo and its subhaloes (see also Zhang et al. 2002). Ma & Boylan-Kolchin show with *N*-body simulations that the dynamical evolution of subhaloes, depending on their mass and concentration, can either steepen or flatten the halo cusp. Thus, the determination of the amount and distribution of DM in cluster galaxies is very relevant also to the problem of the cluster cusp.

As a consequence, the discrepancies found between the observationally determined inner DM profiles and the predictions of CDM models must not necessarily represent a failure of CDM, at least at the cluster scale. Instead, they could reflect our poor understanding of the formation and evolution of galaxies, where the physics of baryons is important. These processes have to be taken into account when predicting the properties of DM haloes of clusters, on scales of a few tens of kiloparsec or smaller. At the same time, our simulations – when interpreted in the context of structure formation (i.e. galaxies considered as subhaloes of DM) – indicate that is quite remarkable to obtain a universal DM profile as a result of successive aggregations,[3] due to the requirement that dynamical friction heating, potential well contraction and mass increase all balance. This detailed balance should be further studied in cosmological simulations.

REFERENCES

Barnes J., White S. D. M., 1984, MNRAS, 211, 753
Bartelmann M., Meneghetti M., 2004, A&A, 418, 413
Bertin G., Liseikina T., Pegoraro F., 2003, A&A, 405, 73
Binney J., 2004, in Ryder S., Pisano D. J., Walker M., Freeman K., eds, Proc. IAU Symp. 220, Dark Matter Galaxies. Astron. Soc. Pac., San Francisco, p. 3
Blumenthal G. R., Faber S. M., Flores R., Primack J. R., 1986, ApJ, 301, 27
Dalal V., Keeton C. R., 2004, preprint (astro-ph/0312072)
de Blok W. J. G., McGaugh S. S., Bosma A., Rubin V. C., 2001, ApJ, 552, L23
Dehnen W., 1993, MNRAS, 265, 250
Dehnen W., 2002, J. Comput. Phys., 179, 27
Dubinski J., 1998, ApJ, 502, 141
El-Zant A., Hoffman Y., Primack J., Combes F., Shlosman I., 2004, ApJ, 607, L75
Gavazzi R., Fort B., Mellier Y., Pellò R., Dantel-Fort M., 2003, A&A, 403, 11
Ghigna S., Moore B., Governato F., Lake G., Quinn T., Stadel J., 2000, ApJ, 544, 616
Gnedin O. Y., Kravtsov A. V., Klypin A. A., Nagai D., 2004, ApJ, submitted (astro-ph/0406247)
Hernquist L., 1990, ApJ, 356, 359
Jesseit R., Naab T., Burkert A., 2002, ApJ, 571, L89
Kazantzidis S., Mayer L., Mastropietro C., Diemand J., Stadel J., Moore B., 2004, ApJ, 608, 663
Kelson D. D., Zabludoff A. I., Williams K. A., Trager S. C., Mulchaey J. S., Bolte M., 2002, ApJ, 576, 720
Kochanek C. S., White M., 2001, ApJ, 559, 531
Lewis A. D., Buote D. A., Stocke J. T., 2003, ApJ, 586, 135
Londrillo P., Nipoti C., Ciotti L., 2003, in Capuzzo-Dolcetta R., ed., Computational Astrophysics in Italy: Methods and Tools. Mem. Soc. Astron. Ital. Suppl., 1, 18
Ma C.-P., Boylan-Kolchin M., 2004, Phys. Rev. Lett., 93, 021301
Merritt D., 1983, ApJ, 264, 24
Mo H. J., Mao S., White S. D. M., 1998, MNRAS, 295, 319

[3] We note that a non-homology effect of successive dissipationless mergings has already been reported by Nipoti et al. (2003a).

Moore B., Governato F., Quinn T., Stadel J., Lake G., 1998, ApJ, 499, L5

Natarajan P., Kneib J.-P., Smail I., 2002, ApJ, 580, L11

Navarro J. F., Frenk C. S., White S. D. M., 1996, ApJ, 462, 563 (NFW)

Navarro J. F. et al., 2004, MNRAS, 349, 1039

Nipoti C., 2003, PhD thesis, Univ. Bologna

Nipoti C., Londrillo P., Ciotti L., 2003a, MNRAS, 342, 501

Nipoti C., Stiavelli M., Ciotti L., Treu T., Rosati P., 2003b, MNRAS, 344, 748 (N03)

Nipoti C., Stiavelli M., Ciotti L., Treu T., Rosati P., 2003c, in Bender R., Renzini A., eds, Proc. ESO–USM–MPE Workshop 'Multiwavelength Mapping of Galaxy Formation and Evolution', in press (astro-ph/0311424)

Ostriker J. P., Tremaine S. D., 1975, ApJ, 202, L13

Power C., Navarro J. F., Jenkins A., Frenk C. S., White S. D. M., Springel V., Stadel J., Quinn T., 2003, MNRAS, 338, 14

Ricotti M., 2003, MNRAS, 344, 1237

Rosati P., della Ceca R., Norman C., Giacconi R., 1998, ApJ, 492, L21

Salucci P., Burkert A., 2000, ApJ, 537, L9

Sand D. J., Treu T., Ellis R. S., 2002, ApJ, 574, L129

Sand D. J., Treu T., Smith G. P., Ellis R. S., 2004, ApJ, 604, 88

Simon J. D., Bolatto A. D., Leroy A., Blitz L., 2003, ApJ, 596, 957

Smith G. P., Kneib J.-P., Ebeling H., Czoske O., Smail I., 2001, ApJ, 552, 493

Spergel D. N., Steinhardt P. J., 2000, Phys. Rev. Lett., 84, 3760

Springel V., Yoshida N., White S. D. M., 2001, New Astron., 6, 79

Subramanian K., Cen R., Ostriker J. P., 2000, ApJ, 538, 528

Treu T., Koopmans L., 2004, ApJ, 611, 739

van den Bosch F. C., Robertson B. E., Dalcanton J. J., de Blok W. J. G., 2000, AJ, 119, 1579

Zhang B., Wyse R. F. G., Stiavelli M., Silk J., 2002, MNRAS, 332, 647

This paper has been typeset from a TEX/LATEX file prepared by the author.